

Jerry Goodisman · Douglas Hagrman · Kirk A. Tacka
Abdul-Kader Souid

Analysis of cytotoxicities of platinum compounds

Received: 3 January 2005 / Accepted: 5 April 2005 / Published online: 19 July 2005
© Springer-Verlag 2005

Abstract Extent of DNA platination, loss of cell viability, DNA fragmentation, and impairment of cellular mitochondrial oxygen consumption are measures of drug cytotoxicity. We measured and compared these effects for cisplatin, oxaliplatin and carboplatin. Because reaction with intracellular thiols may be responsible for drug resistance, we also determined the rates of Pt drug reactions with metallothionein. Jurkat cells were exposed at 37°C to 25 μM Pt drugs for 3 h. Pt-DNA adducts were determined at the end of the incubation period by atomic absorption spectroscopy. Viability, DNA fragmentation, and cellular respiration ($\mu\text{M O}_2/\text{min}/10^6$ cells) were determined 24 h post drug exposure. The average amount of Pt-DNA adducts (Pt atoms/ 10^6 nucleotides) produced by cisplatin was 43.4, by oxaliplatin 4.8 and by carboplatin 1.5. Cisplatin decreased the rate of respiration by $\sim 63\%$ and oxaliplatin by $\sim 37\%$. DNA fragmentation by cisplatin and oxaliplatin was very similar. Carboplatin produced an unnoticeable effect on cellular respiration, and only $\sim 10\%$ of the DNA fragmentation was produced by cisplatin or oxaliplatin. Although, for a given drug, all four measures of cytotoxicity were proportional, this did not hold for comparisons between the drugs. The rate constants ($\text{M}^{-1} \text{s}^{-1}$) for reaction of cisplatin, oxaliplatin and carboplatin with Cd/Zn thionein were 0.75, 0.44 and 0.012,

respectively. For comparison, the rate constants ($\text{M}^{-1} \text{s}^{-1}$) for reaction of cisplatin, oxaliplatin and carboplatin with glutathione were 0.027, 0.038 and 0.0012, respectively. The low reactivity of carboplatin with metallothionein and glutathione suggests that its low cytotoxic activities are not due to reaction of Pt^{2+} with cellular thiols. Despite a tenfold difference in Pt-DNA adducts between cisplatin and oxaliplatin, the cytotoxicities of these compounds are very similar, suggesting that oxaliplatin lesions are more potent than cisplatin lesions. The results demonstrate a large influence of the ligands occupying Pt coordination spheres on the chemical and biologic activities of Pt drugs.

Keywords Cisplatin · Carboplatin · Oxaliplatin · Cd/Zn-thionein · Glutathione · Apoptosis

List of Abbreviations

k_2	Second-order rate constant
k	Zero-order rate constant for cellular respiration
AAS	Atomic absorption spectroscopy
Pd	Phosphor, palladium derivative of <i>meso</i> -tetra-(4-sulfonatophenyl)-tetrabenzoporphyrin

This work was supported by a generous fund from the Paige's Butterfly Run.

J. Goodisman
Department of Chemistry, Syracuse University, 1-014 CST,
Syracuse, NY, 13244 USA

D. Hagrman · K. A. Tacka · A.-K. Souid (✉)
Department of Pediatrics, State University of New York,
Upstate Medical University, 750 East Adams Street,
Syracuse, NY, 13210 USA
E-mail: souida@upstate.edu
Tel.: +1-315-4645294
Fax: +1-315-4647238

Introduction

Pt drugs (cisplatin, carboplatin and oxaliplatin) exert antitumor activity primarily by binding to cellular DNA [11, 22]. These events lead to cell death by apoptosis or necrosis [14, 19, 26, 44, 45, 50]. Apoptosis is executed by a series of cysteine proteases, termed caspases [5, 18]. Caspase activation leads to mitochondrial dysfunction [35] and DNA fragmentation [30, 48]. The mitochondrial perturbation involves opening the permeability transition-pores (PTP), collapsing the electrochemical potential ($\Delta \psi$), releasing cytochrome c and suppressing cellular respiration [4, 25, 44, 45]. In the cytosol, cytochrome c binds to apoptotic protease activating factor-1

(Apaf-1), which activates caspase 9 [27]. The latter activates caspase 3, which executes proteolytic and DNA fragmentation cascades [30, 48]. DNA is initially cleaved to large fragments. Further cuts produce an oligonucleosomal ladder [$\leq 10,000$ base pair (bp)], in multiples of ~ 200 bp. Cell necrosis can also produce similar cellular perturbations.

We recently used a highly sensitive phosphorescence analyzer that measures oxygen concentration $[O_2]$ in solution to explore the impact of cisplatin treatment on cellular respiration [44, 45]. $[O_2]$ in the cell suspensions was determined as a function of time with the aid of Pd (II) *meso*-tetra-(4-sulfonatophenyl)-tetrabenzoporphyrin [42]. The phosphorescence decay of this probe is characterized by a single exponential, with reciprocal of the decay time being linear in $[O_2]$ [15]. Using this method, we showed a linear correlation between DNA platination by cisplatin (measured at the end of 3-h incubation with the drug) and a decreased cellular respiration (measured 24 h post drug exposure). A similar correlation was also found between DNA platination and DNA fragmentation [44].

Resistance to Pt drugs involves numerous mechanisms [21]; an important one seems to be reaction with cellular thiols. Cellular thiols occurring with the highest concentrations (in the mM range) are glutathione (GSH) and metallothionein (MT) [17]. The reaction of Pt drugs with GSH and MT may limit the amount of Pt available for binding to DNA [8, 38, 40, 47]. It has been estimated that only $\sim 1\%$ of Pt that enters the cell binds to nuclear DNA.

The reactions of GSH and MT with cisplatin have been previously studied [2, 7, 16, 17, 23, 33, 38, 51] and the reactions of GSH and MT with carboplatin and oxaliplatin have been recently reported [17]. However, data on the reactions of carboplatin and oxaliplatin with MT are lacking. Carboplatin and oxaliplatin have different ligands occupying the Pt coordination spheres from cisplatin (Fig. 1). Moreover, these newer cisplatin analogs have unique antitumor activity and toxicity profiles [12, 34, 47]. Therefore, their reactions with DNA and MT, as well as induction of apoptosis (measured as

DNA fragmentation and mitochondrial dysfunction) are expected to differ from those of cisplatin.

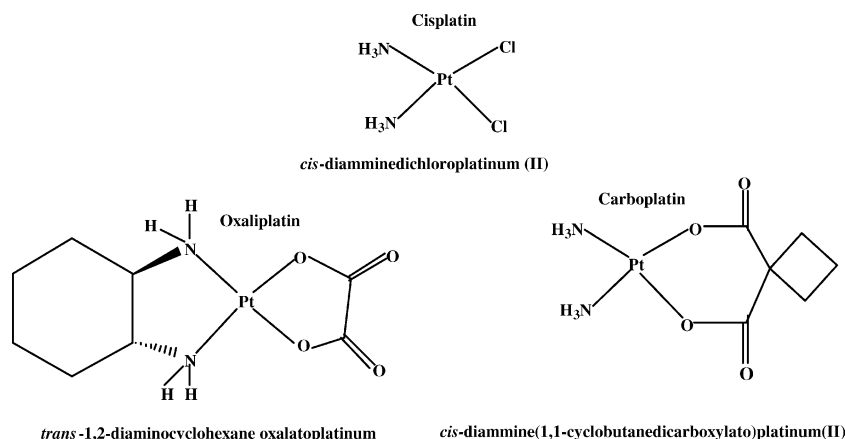
To address these issues, we measured DNA platination, DNA fragmentation and cellular respiration for each Pt drug. Moreover, we determined second-order rate constants for carboplatin and oxaliplatin binding to the naturally occurring Cd/Zn-thionein, under in vitro conditions that mimic those achieved clinically. We used the formulations given to patients, at concentrations that resemble peak plasma Pt levels [6, 9, 12, 28, 32, 43]. For comparisons, it would be reasonable to use concentrations of Pt drugs that gave equal cytotoxicity. However, equal cytotoxicities, as measured by different criteria, require different drug concentrations. Understanding the unique properties of each Pt drug is important for understanding its mechanism of cytotoxicity. Therefore, we use $[Pt\text{ drug}] = 25\text{ }\mu\text{M}$ for all three Pt drugs. The reactions are investigated at $37 \pm 0.1^\circ\text{C}$ and at a pH of 7.4, maintained by 10 mM Hepes or Tris- NO_3 (36). DNA platination and cell viability were determined immediately following drug exposure. Cellular respiration and DNA fragmentation were determined 24 h post drug exposure.

Materials and Methods

Chemicals

Carboplatin (M_R 371.25; lyophilized powder containing equal carboplatin and mannitol by weight) was purchased from Bristol-Myers Squibb Company (Princeton, New Jersey); oxaliplatin (M_R 397.3; lyophilized powder containing equal amounts of oxaliplatin and lactose by weight) was purchased from Sanofi-Synthelabo (Bedford, Ohio); cisplatin (M_R 300.05, 1.0 mg/ml solution, ~ 3.3 mM in 154 mM NaCl) was purchased from Pharmaceutical Partners (Los Angeles, CA); Pd derivative of *meso*-tetra-(4-sulfonatophenyl)-tetrabenzoporphyrin (Pd phosphor, sodium salt, $M_R \sim 1,300$) was purchased from Porphyrin Products, Inc. (Logan, UT); SnakeSkin pleated dialysis tubing (M_R cutoff 3,500 Da) was pur-

Fig. 1 Chemical structures of the Pt compounds studied in the present work



chased from Pierce (Rockford, IL); Pt atomic spectroscopy standard (H_2PtCl_6 , 1 mg/ml in 10% HCl) was purchased from Perkin-Elmer (Norwalk, CT); RPMI-1640 medium with L-glutamine (pH 7.15) were purchased from Mediatech (Herndon, VA); and Cd/Zn-thionein I (from rabbit liver, $M_R \sim 6,000$ Da, 5.0 mg containing 3% Cd and 1% Zn) and remaining reagents were purchased from Sigma-Aldrich (St. Louis, MO).

Solutions

Carboplatin and oxaliplatin were dissolved in dH_2O (10 mg Pt drug per ml = ~ 27 mM and ~ 12.6 mM, respectively) immediately prior to use. Dihexylammonium acetate (2.5 mM) HPLC solvent A was prepared in the hood by the addition of 590 μl of 4.24 M dihexylamine and 144 μl of 17.4 M glacial acetic acid to each liter of dH_2O . The pH was adjusted to ~ 7.0 by small additions of dihexylamine or acetic acid. The solution was continuously stirred. Pd phosphor was dissolved in dH_2O (2.5 mg/ml or ~ 2.0 mM) and stored in the refrigerator for \sim one week. Cd/Zn-thionein was dissolved in 1.0 ml dH_2O and stored at -20°C . Its final concentration was determined as apo-thionein as described previously [16].

Cells

Cells of the human T cell lymphoma cell line, Jurkat, (American Type Culture Collection, Manassas, VA) were maintained in suspension culture under a fully humidified atmosphere containing 5% CO_2 at 37°C . The medium was RPMI-1640 supplemented with 10% (v/v) FBS, 100 $\mu\text{g}/\text{ml}$ streptomycin, 100 IU/ml penicillin and 2.0 mM L-glutamine. Cell count and cell viability were determined by light microscopy immediately prior to all experimental measurements, using a hemacytometer under standard trypan blue staining conditions [1].

Cellular incubations with Pt drugs

Incubations were carried out in medium plus 10% fetal bovine serum at 37°C . Cells in logarithmic growth ($\sim 10^7$ /condition) were exposed to 25 μM of each Pt drug for 3 h. At the end of incubation periods, the cells were collected by centrifugation, maintained in culture (drug-free medium) and analyzed 24 h later.

Cell viability

Cell viability measurements were performed using a Neubauer hemacytometer with two counting chambers. Trypan blue was used to distinguish between viable and non-viable cells. Only non-viable cells absorb the dye, appearing blue and asymmetric under the microscope.

Cellular mitochondrial oxygen consumption

Cellular respiration was measured at RT in sealed vials. The substrate was glucose. The cells were suspended in 0.5 ml of Pd phosphor solution [RPMI medium (contains ~ 6.0 mM Na_2HPO_4 and 10 mM glucose) supplemented with 2 μM Pd phosphor and 3% fat-free bovine serum albumin (final pH, ~ 7.5)]. The concentration of oxygen $[\text{O}_2]$ in the solution was measured as a function of time, using the phosphorescence probe Pd (II) *meso*-tetra-(4-sulfonatophenyl)-tetrabenzoporphyrin as described in [15, 42, 44, 45].

The rate of cellular mitochondrial oxygen consumption ($\mu\text{M O}_2 \text{ min}^{-1}$) was calculated as the negative slope of the linear portion of the $[\text{O}_2]$ versus time curves. The value of k (zero-order rate constant) was set equal to the negative slope of each curve divided by the number of cells ($\times 10^6$) in each sample (as shown in Fig. 2). The rate of oxygen consumption for the Pd phosphor solution without cells was (mean \pm SD) $0.28 \pm 0.05 \mu\text{M min}^{-1}$, and for $\sim 10^7$ cells incubated with rotenone (50 μM at 37°C for 1 h, inhibits Complex I of the respiratory chain) was $0.36 \pm 0.16 \mu\text{M min}^{-1}$, confirming O_2 was consumed in the respiratory chain.

DNA fragmentation

DNA fragments were extracted, separated on gel electrophoresis, stained and quantitated as shown in Fig. 3 and previously described [13, 44, 45]. Intensities corre-

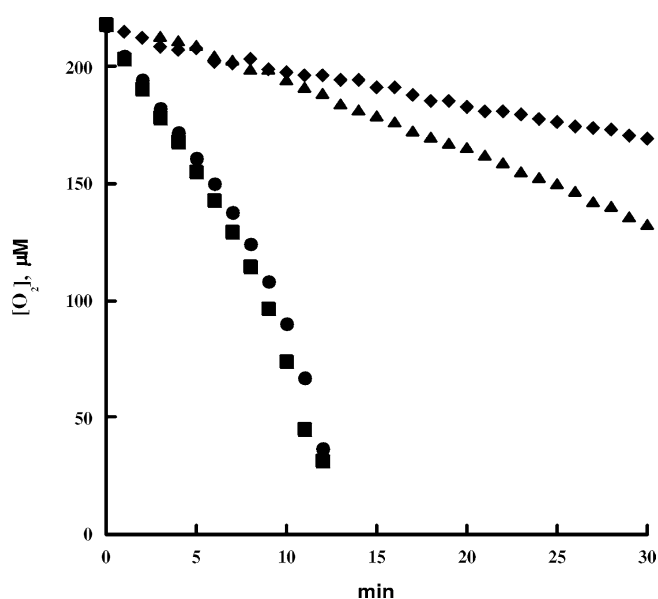


Fig. 2 Oxygen concentration versus time, showing effects of Pt drugs on cellular respiration. Jurkat cells were incubated for 3 h without (circles) and with 25 μM cisplatin (diamonds), oxaliplatin (triangles) or carboplatin (squares), and measured ~ 24 h post drug exposure. The respiration rate constants k , determined from negative slopes of the curves ($r > 0.99$), are expressed in $\mu\text{M O}_2$ per min per 10^6 cells and shown in Table 1

sponding to fragments < 2 kbp in length were measured using Sigma Scan (Jandel Scientific, Inc.).

PT-DNA adducts

Cellular DNA was extracted immediately following 3-h incubation with 25 or 50 μM of Pt drugs. Pt-DNA adducts were determined by atomic absorption spectroscopy (AAS) as described in [40, 44, 45].

Chemical reactions of Pt drugs with MT

Solutions containing Cd/Zn-thionein (83 μmol) and 10 mM Hepes or Tris- NO_3 (final volume 1.0 ml with dH_2O and final pH 7.4) were placed in the SnakeSkin pleated dialysis tubing, and dialyzed at 4°C for ~16 h against two changes of 2 l of 10 mM Hepes or Tris- NO_3 (pH, ~7.4). At the end of the dialysis procedure, the Cd/Zn-thionein (inside solution) was used immediately for the following chemical reactions (all of which were carried out at $37 \pm 0.1^\circ\text{C}$).

The reaction mixture contained Pt drug, dialyzed Cd/Zn-thionein and 4.62 mM NaCl (final pH ~7.4 and final volume 1.0 ml). The control mixture contained dialyzed Cd/Zn-thionein and 4.62 mM NaCl, without Pt drug. Another control mixture contained Pt drug, 4.62 mM NaCl and the outside solution (instead of dialyzed Cd/Zn-thionein).

HPLC-UV

Analysis was performed on the Beckman HPLC system (automated injector model 507e, pump model 125, and UV detector model 166) as described in [7, 16, 17]. UV detection at 260 nm was used. Solvent A was 2.5 mM DHAA in dH_2O and solvent B HPLC-grade methanol. The 4.6 \times 250 mm Beckman Ultrasphere IP column was operated at room temperature at 0.5 ml/min. The chromatography procedure employed linear gradients as follows: 0 min, 10% B; 5 min, 10% B; 20 min, 75% B; 40 min, 100% B; 45 min, 100% B; 46 min, 10% B; 60 min, re-inject. The injection volume was 50 μl . Eluates containing Pt were collected and analyzed on the AAS.

AAS

Pt analysis was performed on the graphite furnace of a Shimadzu AAS (Model, AA-6800), with an ist (Imaging and Sensing Technology, Horseheads, NY) hollow cathode Pt lamp, deuterium arc background correction, and pyrolytically coated graphite tubes [7, 40]. The instrument operated at a lamp current of 14 mA, wavelength of 266 nm, and a slit width of 0.5 nm. The graphite tubes were changed after ~100 ignitions. Argon gas and tap water flowed through the furnace hoses. The injection volume was 20 μl . The furnace program used sequential drying (70°C for 10 s, 90°C for 10 s, and 120°C for 10 s), charring (250°C for 10 s and 800°C for 25 s), cooling (30°C for 20 s), atomization (2,600°C for 5 s) and cleaning (~3,000°C for 5 s) phases. A standard solution was freshly made by serial dilutions of the Pt atomic absorption standard stock (1 mg/ml of H_2PtCl_6) in dH_2O plus 1% HNO_3 (v/v). A calibration curve (using 0.01 mg/l or 513 nM solution) was generated prior to each measurement and proved to be linear from 0 pmol to 10 pmol ($r > 0.99$). The lower limit of detection was ~20 pg atomic Pt (~0.1 pmol). A background reading of ~0.005 optical density (for dH_2O) was subtracted from each of the determinations [7, 40].

Kinetics of Pt drug binding to Cd/Zn-thionein

The reaction was assumed to be of second order, with one Pt reacting with one Cd/Zn-thionein. This must be the case at the beginning of the reaction, when most of the Cd/Zn-thionein has not reacted with Pt.

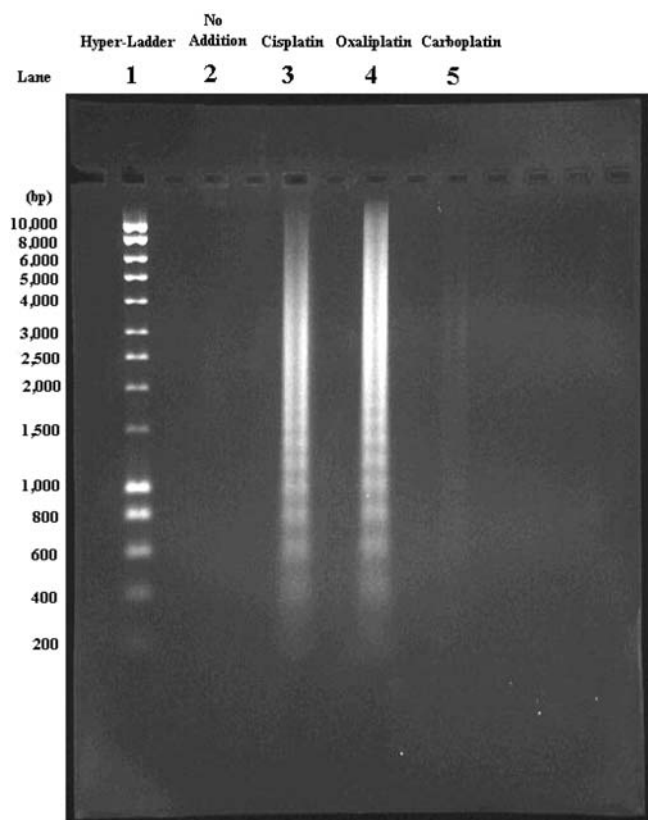


Fig. 3 Stained electrophoresis gel, showing effects of Pt drugs on DNA fragmentation. Jurkat cells ($\sim 10^7$ cells per condition) were incubated for 3 h with and without 25 μM Pt drugs. The cells were then maintained in drug-free medium for ~24 h. The net intensities corresponding to small DNA fragments were measured. Results from three independent experiments are shown in Table 1

The rates of carboplatin and oxaliplatin reactions with Cd/Zn-thionein were thus analyzed using the second-order rate equation, exactly as done for the cisplatin reaction [16]. If $[\text{Pt drug}]_0$ and $[\text{MT}]_0$ denote the initial concentrations of Pt drug and MT, respectively, and $[\text{Pt drug}]$ and $[\text{MT}]$ denote their concentrations at t ,

$$\ln\left(\frac{[\text{Pt drug}][\text{MT}]_0}{[\text{MT}][\text{Pt drug}]_0}\right) = k_2([\text{Pt drug}]_0 - [\text{MT}]_0)t. \quad (1)$$

The Pt drug concentrations at time t were determined from eluates corresponding to the free (unbound) drug. The concentration of Pt-thionein product formed at t , $[\text{product}]$, was calculated as the difference between $[\text{Pt drug}]_0$ and $[\text{Pt drug}]$ and then $[\text{MT}]$ was calculated as $[\text{MT}]_0 - [\text{product}]$. The change in $[\text{Pt drug}]$ in the control mixture (see above) was subtracted from the change in the reaction mixture when the former was appreciable.

Carboplatin pharmacokinetics

The plasma Pt concentrations were determined as described in [43]. The study was approved by the institutional review board (State University of New York, Upstate Medical University) for the protection of human subjects. Informed consent was obtained from each patient.

Results

PT-DNA adducts

Pt-DNA adducts were measured at the end of 3-h incubation (at 37°C) with 25 μM Pt drugs. The results for the three compounds, and for background (incubation in the absence of drug) are shown in Table 1. After subtracting the background, DNA platination by cisplatin was 43.4 (100%) per 10^6 nucleotides, by oxaliplatin 4.8 (~11%) per 10^6 nucleotides and by carboplatin 1.5 (~4%) per 10^6 nucleotides.

Pt-DNA adducts were also measured at the end of 3-h incubation (at 37°C) with 50 μM Pt drugs. After subtracting the background, DNA platination by cisplatin was (mean \pm SD, $n=3$) 377 ± 24 per 10^6 nucleotides, by oxaliplatin 231 ± 74 per 10^6 nucleotides, and by carboplatin 38 ± 16 per 10^6 nucleotides.

Viability

Cell viability was 96% for the control, with no exposure to drug (Table 1). It decreased to 72% with cisplatin treatment, 85% with oxaliplatin treatment and 94% with carboplatin treatment (close to the value for the control). The relative growth (cell counts reached by the treated culture divided by cell counts reached by the untreated culture for each condition) in the presence of cisplatin was 0.53, oxaliplatin 0.72 and carboplatin 0.83.

Cellular respiration

Cellular mitochondrial oxygen consumption was measured 24 h post exposure (at 37°C) to 25 μM Pt drug, and compared with oxygen consumption for cells not exposed to drug. The rate of oxygen consumption, k , was the negative slope of a curve of $[\text{O}_2]$ versus t , divided by the number of cells in millions. The average values of k for three independent experiments, including that of Fig. 2, are summarized in Table 1. Cisplatin decreased the value of k by ~63% and oxaliplatin by ~37%. Carboplatin, on the other hand, had no effect on cellular respiration within the stated experimental uncertainty.

DNA fragmentation

DNA fragmentation (intensities corresponding to DNA fragments produced by apoptosis) was measured 24 h post exposure (at 37°C) to 25 μM Pt drug. As shown in Table 1 and Fig. 3, the net intensities (after subtraction of control-lane intensities) were almost the same for the cisplatin and oxaliplatin treatments. In contrast, the carboplatin treatment produced DNA fragmentation only ~10% of that of cisplatin or oxaliplatin.

Reaction of carboplatin with Cd/Zn-thionein

Representative HPLC runs of the reaction mixture at 1.17 h and 50.28 h are shown in Fig. 4. The decrease in intensity of the peak near retention time $t_R \sim 8$ min is evident. The Pt contents of the eluates with $7 < t_R < 11$ min (corresponding to unbound carboplatin) are shown in Fig. 5a for the reaction mixture (squares) and for the control mixture (circles).

Table 1 Cytotoxicities of the Pt compounds

Addition	Pt-DNA	Viability	Value of k	Fragment intensity
None	4.5 ± 4.3 (4)	96 ± 1.2 (3)	0.30 ± 0.03 (3)	7.7 ± 4.6 (3)
Cisplatin	47.9 ± 15.5 (4)	72 ± 7.5 (3)	0.11 ± 0.03 (3)	33.1 ± 5.6 (3)
Oxaliplatin	9.3 ± 2.5 (4)	85 ± 5.1 (3)	0.19 ± 0.08 (3)	30.2 ± 5.4 (3)
Carboplatin	6.0 ± 1.6 (4)	94 ± 2.1 (3)	0.33 ± 0.05 (3)	8.4 ± 2.5 (3)

Jurkat cells were incubated at 37°C for 3 h with no addition or with the addition of 25 μM Pt drug. DNA platination (Pt/ 10^6 nt) was determined at the end of the incubation period. Viability (%), cellular mitochondrial oxygen consumption (k , in $\mu\text{M O}_2$ per min per 10^6 cells) and DNA fragment intensity (arbitrary units, $\div 10^3$) were determined 24 h post drug exposure. The numbers are mean \pm SD (n)

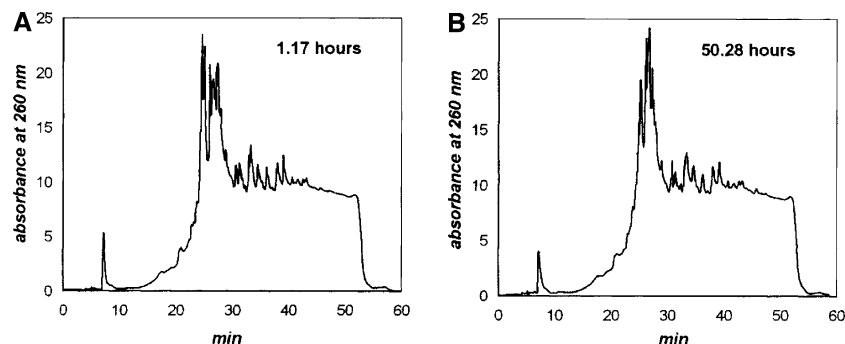


Fig. 4 Chromatograms of the reaction of carboplatin with Cd/Zn-thionein (ultraviolet absorbance vs. retention time). Chromatograms of the reaction mixture (135 μM carboplatin, 48 μM Cd/Zn-thionein, 10 mM Hepes and 4.62 mM NaCl) are shown at 1.17 h, panel a, and 50.28 h, panel b. Pt contents of eluates with $7 < t_R < 11$ min (corresponding to unbound carboplatin) are shown in Fig. 5, panel a. The areas of the corresponding HPLC peaks are shown in Fig. 5, panel b

The areas of the peaks corresponding to unbound carboplatin ($t_R \sim 8$ min) are similarly shown in Fig. 5b. The recovery of carboplatin from the eluate with $7 < t_R < 11$ min at reaction time zero was 126 μM ($\sim 93\%$). Linear regression for the control mixture results in Fig. 5a gave a slope of $0.088 \pm 0.187 \mu\text{M h}^{-1}$, that is, zero within the standard error, indicating no appreciable reaction with the buffer. For the reaction mixture, the slope was definitely negative, $-0.303 \pm 0.170 \mu\text{M h}^{-1}$. Linear regression on the peak areas for the control mixture showed zero slope within the standard error ($-0.0002 \pm 0.0021 \text{ h}^{-1}$), whereas for the reaction mixture the slope was definitely negative ($-0.0043 \pm 0.0012 \text{ h}^{-1}$).

The reaction was very slow. For example, the concentration of unbound carboplatin, 126 μM at 0 h, was

108 μM (86%) at 27 h. The reaction mixture was dialyzed (see Methods) at reaction time 20 h. The Pt content in the inside solution was only 2.87 μM (2.3% of the total Pt), confirming that only a small fraction of carboplatin was bound to Cd/Zn-thionein. Because the rate is so slow, the rate constants were determined from the initial slopes rather than from the full second-order expression. The relative slopes (slopes divided by the y-intercepts) were the same for the Pt contents and peak areas (Fig. 5a, b, squares), 0.00259 and 0.00252, respectively. Since the slopes for the control mixture were zero in both determinations (Fig. 5a, b, circles), correction for carboplatin reaction with the buffer was not necessary. The initial rates were $0.303 \pm 0.170 \mu\text{M h}^{-1}$ from the Pt contents (Fig. 5a) and $0.340 \pm 0.096 \mu\text{M h}^{-1}$ from the peak areas (Fig. 5b). The value of k_2 for carboplatin binding to Zn/Cd-thionein was calculated, assuming second-order kinetics, to be $(1.30 \pm 0.73) \times 10^{-2} \text{ M}^{-1} \text{ s}^{-1}$ from the Pt contents and $(1.46 \pm 0.41) \times 10^{-2} \text{ M}^{-1} \text{ s}^{-1}$ from the peak areas.

The experiment was repeated using Tris- NO_3 buffer and 61 μM MT (instead of 48 μM). The Pt contents of the eluates with $7 < t_R < 11$ min and the areas of the peaks with $t_R \sim 7.2$ min were measured out to 24 h. The recovery of carboplatin from the eluate with $7 < t_R < 11$ min at reaction time zero was $\sim 88\%$. Linear least-square fits of Pt contents and peak areas versus time gave relative slopes of -0.0027 ± 0.0007 and -0.0040 ± 0.0006 , indicating that the two experiments measured the same rate process. The average of the two rates was 0.44 $\mu\text{M/h}$, 1.37 times the average from the experiment of Fig. 5, 0.32 $\mu\text{M/h}$. Since the ratio of [MT] is $61/48 = 1.27$, the measured reaction is of first order in MT. The rate constants, calculated from the initial rates assuming mixed second-order kinetics, are

Fig. 5 Kinetics of carboplatin reaction with Cd/Zn-thionein in Hepes buffer. The reaction mixture (squares) contained 135 μM carboplatin, 48 μM Cd/Zn-thionein, 10 mM Hepes and 4.62 mM NaCl (pH 7.4). The control mixture (circles) contained 135 μM carboplatin, 10 mM Hepes and 4.62 mM NaCl. Panel a shows Pt contents (determined by AAS) of the eluates with $7 < t_R < 11$ min, corresponding to unbound carboplatin. Panel b shows the areas of peaks with $t_R \sim 7.2$ min, corresponding to unbound carboplatin. Values of k_2 , calculated from the initial slopes, were $(1.30 \pm 0.73) \times 10^{-2} \text{ M}^{-1} \text{ s}^{-1}$ from panel a and $k_2 = (1.46 \pm 0.41) \times 10^{-2} \text{ M}^{-1} \text{ s}^{-1}$ from panel b

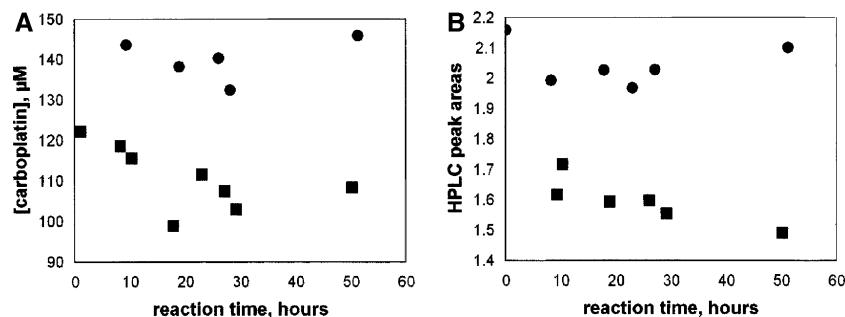
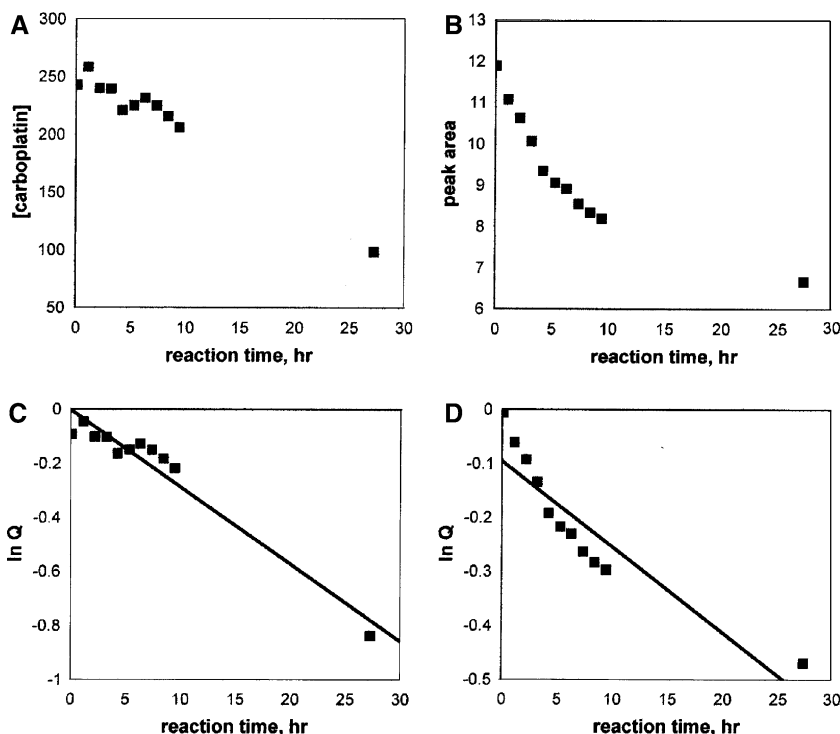


Fig. 6 Kinetics of carboplatin reaction with Cd/Zn thionein in Hepes buffer. The reaction contained 270 μM carboplatin, 1.06 mM Cd/Zn thionein, 10 mM Hepes and 4.62 mM NaCl. The amount of unbound carboplatin is shown as a function of time. Panel a shows Pt contents of the eluates with $7 < t_R < 11$ min; panel b shows the areas of HPLC peaks with $t_R \sim 7.2$ min. The data of panel a are analyzed assuming second-order kinetics, giving $\ln Q$ versus t shown in panel c with least-square linear fit, from which $k_2 = 0.01002 \text{ M}^{-1} \text{ s}^{-1}$. The data of panel b are analyzed similarly, giving $\ln Q$ versus t shown in panel d with least-square linear fit, from which $k_2 = 0.0056 \text{ M}^{-1} \text{ s}^{-1}$.



$k_2 = (1.12 \pm 0.30) \times 10^{-2} \text{ M}^{-1} \text{ s}^{-1}$ from the Pt contents and $k_2 = (1.83 \pm 0.27) \times 10^{-2} \text{ M}^{-1} \text{ s}^{-1}$ from the peak areas. Thus, rate constants from the experiments in Tris- NO_3 buffer were the same as those from the experiments in Hepes buffer within the stated standard deviations.

Another experiment used 270 μM carboplatin and 1.06 mM Cd/Zn-thionein, in 10 mM Hepes buffer. The measured Pt concentrations and HPLC peak areas are shown in Fig. 6 (panels a and b, respectively). From the first ten points in panel a, we obtain an initial rate of $(4.22 \pm 0.27) \mu\text{M/h}$ and from the first ten points in panel b $(9.15 \pm 0.78) \mu\text{M/h}$. These are ~ 13 and ~ 29 times the average initial rate from the results of Fig. 5, $0.32 \mu\text{M/h}$. The ratio of initial concentrations is $(270/135)(1060/48) \sim 44$, confirming that we have a mixed second-order reaction. Since a large fraction of the Pt is used up in this case, the data can be analyzed using the full second-order kinetics expression (Eq. 1) rather than initial slopes. Values of $\ln(Q)$ calculated from Pt concentrations are shown in panel c along with the linear fit, the slope of which, -0.0285 , yields $k_2 = 0.010 \text{ M}^{-1} \text{ s}^{-1}$. Values of $\ln(Q)$ calculated from peak areas are shown in panel d with the linear fit; the slope of -0.0159 yields $k_2 = 0.0056 \text{ M}^{-1} \text{ s}^{-1}$. This is well below the other values, probably because an error in the last time point has a disproportionate effect. Nevertheless, we average all six independent experiments to obtain $k_2 = 0.0121 \pm 0.0039 \text{ M}^{-1} \text{ s}^{-1}$ (mean \pm standard deviation), Table 2.

The binding of carboplatin to Cd/Zn-thionein with the former present in excess was investigated using dialysis. The reaction mixture, containing 135 μM car-

boplatin, 27.7 μM Cd/Zn-thionein, 10 mM Hepes and 4.62 mM NaCl, was incubated at 37°C for ~ 70 h. At the end of the incubation period, the mixture was dialyzed as described in Methods. The concentration of Pt in the dialyzed solution was $5.2 \mu\text{M}$, showing that one MT can bind at least 5 Pt atoms. Thus, the reaction rate is proportional to the MT concentration only in the early stages, so that the method of initial rates is a more reliable way of determining k_2 .

Reaction of oxaliplatin with Cd/Zn-thionein.

The reaction mixture contained 135 μM oxaliplatin, 353 μM Cd/Zn-thionein, 10 mM Hepes and 4.62 mM NaCl (pH ~ 7.4). The control mixture was identical except for having no thionein. Representative HPLC runs of the control mixture at 0 h and of the reaction mixture at 1.08 h are shown in Fig. 7a and b, respectively. The

Table 2 Rate constants (k_2), mean \pm SD (n) for cisplatin, oxaliplatin and carboplatin binding to Cd/Zn-thionein and GSH

Pt drug	Cd/Zn-thionein ($\text{M}^{-1} \text{ s}^{-1}$)	GSH ($\text{M}^{-1} \text{ s}^{-1}$)
Cisplatin	0.75 ± 0.03 (3)	0.027 ± 0.0006 (2)
Oxaliplatin	0.44 ± 0.1 (2)	0.039
Carboplatin	0.0121 ± 0.0039 (6)	0.0017 ± 0.00037 (4)

The value of k_2 for cisplatin reaction with Cd/Zn-thionein is from [7, 17]. The values of k_2 for oxaliplatin and carboplatin reactions with Cd/Zn-thionein are determined in the present study. The values of k_2 for Pt drug reactions with GSH are from [16]

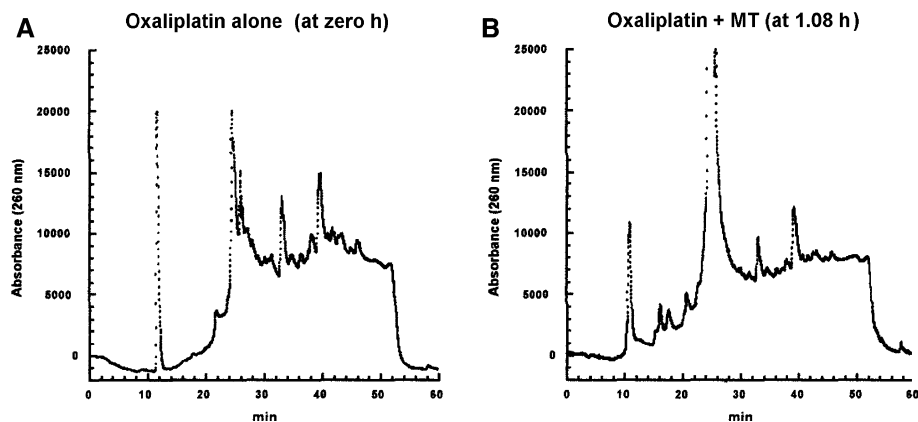
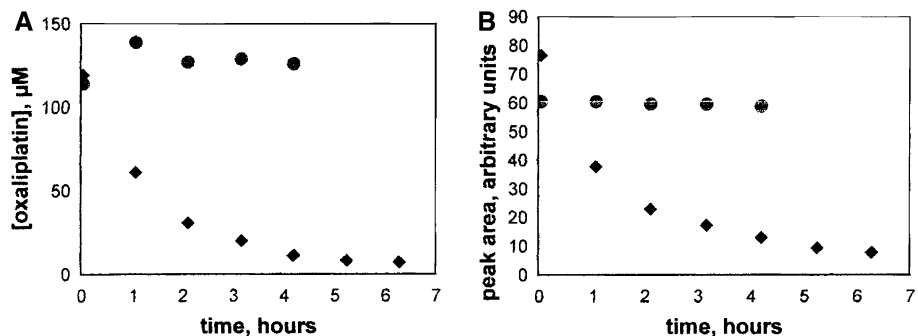


Fig. 7 Chromatograms of the reaction of oxaliplatin with Cd/Zn-thionein. Panel a shows the HPLC for the control mixture (135 μM oxaliplatin, 10 mM Hepes and 4.62 mM NaCl) at 0 h and panel b shows the HPLC for the reaction mixture (135 μM oxaliplatin, 353 μM Cd/Zn-thionein, 10 mM Hepes and 4.62 mM NaCl) at 1.08 h. Retention time (t_R) for oxaliplatin was ~ 11 min. Pt contents of the eluates with $9 < t_R < 13$ min, corresponding to unbound oxaliplatin, are shown in Fig. 8, panel a; areas of corresponding HPLC peaks are shown in Fig. 8, panel b

decrease in intensity of the peak near $t_R \sim 11$ min is evident.

The Pt contents of eluates with $9 < t_R < 13$ min (corresponding to unbound oxaliplatin) are shown in Fig. 8a for the reaction mixture (diamonds) and for the control mixture (circles). The areas of peaks corresponding to unbound oxaliplatin ($t_R \sim 11$ min) are shown in Fig. 8b for the reaction mixture (diamonds) and for the control mixture (circles). The recovery of oxaliplatin from the eluate with $9 < t_R < 13$ min at reaction time zero was $\sim 88\%$. Fitting the Pt contents and peak areas (Fig. 8, diamonds) to exponentials Ae^{-bt} gave $b = 0.46$ and

Fig. 8 Kinetics of oxaliplatin reaction with Cd/Zn-thionein in Hepes buffer. The reaction mixture (diamonds) contained 135 μM oxaliplatin, 353 μM Cd/Zn-thionein, 10 mM Hepes and 4.62 mM NaCl (pH 7.4). The control mixture (circles) contained 135 μM oxaliplatin, 10 mM Hepes and 4.62 mM NaCl. Panel a shows AAS-determined Pt contents of the eluates with $11 < t_R < 13$ min, corresponding to unbound oxaliplatin. Panel b shows the areas of HPLC peaks with $t_R \sim 11$ min, corresponding to unbound oxaliplatin. The value of k_2 calculated from the data of Panel a was $0.51 \text{ M}^{-1} \text{ s}^{-1}$, and the value calculated from the data of Panel b was $0.37 \text{ M}^{-1} \text{ s}^{-1}$



$b = 0.35$, respectively. This showed that both Pt contents and peak areas could be used to monitor the reaction. The zero slopes for the control mixture in both determinations (Fig. 8, circles) made subtraction to correct for oxaliplatin reaction with the buffer unnecessary.

The value of k_2 for oxaliplatin binding to Zn/Cd-thionein was calculated, using (Eq. 1), as $0.51 \text{ M}^{-1} \text{ s}^{-1}$ from the Pt contents (Fig. 8a, diamonds) and $0.37 \text{ M}^{-1} \text{ s}^{-1}$ from the peak areas (Fig. 8b, diamonds), Table 2. The reaction mixture was dialyzed after 7 h. Pt content in the inside solution was $\sim 135 \mu\text{M}$, confirming that all of the oxaliplatin was bound to Cd/Zn-thionein. This is consistent with the plots of Fig. 8, which show that the amount of unreacted oxaliplatin is essentially zero after 7 h.

Pharmacokinetics of carboplatin

The pharmacokinetics of carboplatin was determined in four patients. The C_{max} of free plasma Pt for the three patients who received standard doses of carboplatin at $80\text{--}175 \text{ mg/m}^2$ was $31.3 \pm 8.0 \mu\text{M}$, and for the one patient who received “a high dose” of carboplatin at $\sim 540 \text{ mg/m}^2$ was $216 \mu\text{M}$. The $t_{1/2}$ was 49.1 ± 5.0 min. Thus, $\sim 25 \mu\text{M}$ carboplatin concentration (used as a measure of drug-induced cytotoxicities) mimics clinical levels. For comparison, the C_{max} of free plasma Pt for the 19 patients who received cisplatin at 30 mg/m^2 was $4.5 \pm 1.6 \mu\text{M}$ and the $t_{1/2}$ was 25.4 ± 5.4 min [43]. The C_{max} of free plasma Pt for patients who received oxa-

liplatin at 85 mg/m^2 was $3.6 \pm 0.5 \text{ }\mu\text{M}$ and the $t_{1/2}$ was $\sim 14.1 \text{ min}$ [9].

Discussion

We have used four quantitative measures of cell damage to compare the impact of Pt drug treatments on tumors. These measurements are: (1) reaction with cellular DNA to form Pt-DNA adducts, (2) loss of cell viability, (3) impairment of cellular respiration, and (4) DNA fragmentation. The results are shown in Table 1. Moreover, we have determined the rate constants for oxaliplatin and carboplatin reactions with Cd/Zn-thionein (Table 2). The rate constants for cisplatin reaction with Cd/Zn-thionein and Pt drug reactions with GSH are also shown for comparison [6, 16, 17], Table 2.

For a graphical comparison of the four measures of cell damage, Fig. 9 shows the number of Pt-DNA adducts per million nt (1), the loss of cell viability (2, calculated as the difference between treated and untreated cells), the loss of cellular respiration (3) and the induction of DNA fragmentation (4, calculated as the difference in the intensities of DNA fragments for treated and untreated cells). Although the order of toxicities is cisplatin > oxaliplatin > carboplatin by any of the four measures, there are striking quantitative differences between them. This makes it impossible to compare the drugs at concentrations that give equal cytotoxicity, and makes it necessary to use equal drug concentrations for our comparisons.

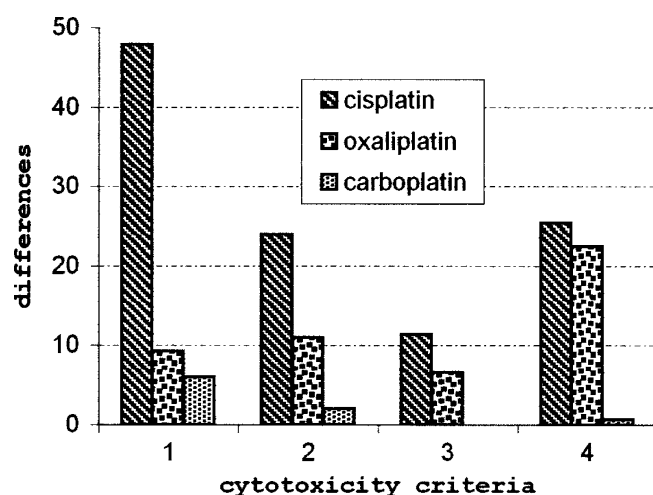


Fig. 9 Comparisons of cytotoxicities of the three Pt drugs by four criteria. 1 number of Pt-DNA adducts/ 10^6 nt; 2 percent loss of viability (untreated minus treated cells); 3 loss of cellular respiration (k for untreated cells minus k for treated cells in $\mu\text{M O}_2/\text{h}/10^6$ cells); 4 intensity of DNA fragments for treated cells minus intensity for untreated cells (arbitrary units)

Thus, despite a \sim tenfold difference in the amount of DNA platination by cisplatin and oxaliplatin, the impairment of cellular respiration and the intensity of DNA fragmentation are similar for the two drugs. One possible explanation for these results is that oxaliplatin lesions are more cytotoxic. This is consistent with data showing that the extent and specificity of replicative bypass are influenced by the carrier ligand of Pt adducts [46]. Carboplatin treatment, on the other hand, produced low levels of DNA platination, loss of cell viability and DNA fragmentation.

Overall, our findings are consistent with the reported ~ 100 -fold difference between cisplatin and carboplatin reactions with DNA [22]. This demonstrates the influence of the ligands occupying the Pt coordination sphere on reaction with DNA and induction of cell apoptosis or necrosis. The results also suggest that the processes leading to drug-induced cell death may differ for different Pt drugs.

As previously shown, a minor structural change in the amine group can lead to a major change in the chemical reactivity of the Pt drugs (Fig. 1) [3]. A steric hindrance may explain the slow reactivity of carboplatin with DNA [31]. The six-membered ring formed between the Pt and the bi-dentate ligand (1,1-cyclobutanedicarboxylato) of carboplatin adopts a configuration that forces the cyclobutane moiety to reside in an axial position of the Pt coordination sphere, which blocks a nucleophile from reaching the Pt(II). The strain in the five-membered ring of oxaliplatin is rapidly relieved by a nucleophilic attack on Pt(II).

It is known that aquation of cisplatin occurs outside the cell, and is followed by a rapid passage of the chloro-aquo species through the membrane of Jurkat cells [45]. However, to our knowledge, similar data for oxaliplatin and carboplatin are not available, although the aquation rate of carboplatin seems to be two orders of magnitude slower than that of cisplatin. Thus, the values of Pt-DNA adducts (Table 1) are not adjusted for a presumed unique cellular uptake of each Pt compound. Moreover, the results in Table 1 do not assume a saturated uptake for each Pt drug by 3 h. We also showed that $\sim 93\%$ of Pt/DNA adducts are removed after incubating cells in drug-free media for 2 h [40]. Therefore, Pt/DNA adducts (Table 1) are measured at the end of the incubation period with the drug.

By trapping Pt^{2+} , cellular thiols (especially GSH and MT) can influence the amount of Pt reaching DNA [49]. When cellular thiols are blocked with *N*-ethylmaleimide, DNA platination by cisplatin increases \sim eightfold [40]. We previously studied the reactions of Pt drugs with GSH [7, 17] and the reaction of cisplatin with MT [16]. In the current study, we describe the reactions of oxaliplatin and carboplatin with MT. The results of all measurements are shown in Table 2.

The Cd/Zn-thionein protein can be saturated with seven Cd, Zn or Pt [16], but the reaction is second order in its initial stages. Thus, we analyzed the reactions according to mixed second-order kinetics. The second-

order rate constant for cisplatin binding to Cd/Zn-thionein ($0.75 \pm 0.06 \text{ M}^{-1} \text{ s}^{-1}$) is very similar to that of Cd₇-thionein ($0.53 \pm 0.03 \text{ M}^{-1} \text{ s}^{-1}$) and Zn₇-thionein ($0.65 \pm 0.03 \text{ M}^{-1} \text{ s}^{-1}$) [16], confirming that Pt can rapidly displace bound Zn and Cd. The rate constants were calculated from disappearance of free (unbound) Pt drugs from the reaction mixtures rather than from appearance of Pt-thionein products. This measure was necessary because the amount of Pt in eluates corresponding to the products was less than the decrease of Pt in eluates corresponding to the free drugs. Possible explanations for this are that some products are trapped in the column or unstable. Each reaction was run simultaneously with a control (identical mixture without Cd/Zn-thionein). Drug decay in the control mixtures was always negligible, showing that loss of Pt in eluates corresponding to the free drugs results from drug binding to Cd/Zn-thionein (rather than drug hydrolysis or reaction with the buffer). At the end of the incubation periods, the remaining reaction mixtures were dialyzed and the Pt contents in the inside solutions were determined by AAS. For the oxaliplatin reaction with Cd/Zn-thionein, all Pt was recovered, confirming that all the oxaliplatin was bound to Cd/Zn-thionein. In contrast, for the carboplatin reaction with Cd/Zn-thionein, only ~4% of the Pt was recovered, and only a small fraction of the Pt was lost from the parent carboplatin peak, even at very long reaction times. The slowness of the reaction made it necessary to obtain k_2 from initial rates rather than from the full second-order kinetic expression. Carboplatin binding to GSH is also slow, 22-fold slower than cisplatin binding (Table 2), suggesting that the drug generally reacts poorly with thiols [22]. Steric hindrance may explain the slow reactivity [31]. In contrast, rates of oxaliplatin reactions with Cd/Zn-thionein and GSH are similar to those for cisplatin [10]. For example, oxaliplatin binding to GSH is 1.4-fold faster than that of cisplatin (Table 2) [17].

The binding of Pt drugs to Cd/Zn-thionein is compared using identical in vitro conditions. One can always question whether in vitro measurements are relevant to intracellular conditions, so that in vivo measurements should be done if possible. However, ratios of rate constants are likely to carry over from in vitro to in vivo, even if absolute values do not.

It has been reported [29, 39, 41] that MT plays roles in cell resistance other than as a Pt-blocker. Nevertheless, the limiting, by cellular thiols, of the amount of Pt drug available to bind to DNA certainly contributes to drug resistance. Therefore, Pt agents like carboplatin that react less well with cellular thiols may be more effective in tumors that over-express GSH and/or MT, and in tumors in which these thiols are induced by prior exposure to Pt drugs.

The differences in Pt drug activities (Tables 1, 2) demonstrate a large influence of the ligands occupying the Pt coordination spheres [10, 22]. These findings provide information which should be helpful in designing more potent Pt compounds.

References

- Allison DC, Ridolpho P (1980) Use of a trypan blue assay to measure the deoxyribonucleic acid content and radioactive labeling of viable cells. *J Histochem Cytochem* 28:700–703
- Berners-Price SJ, Kuchel PW (1990) Reaction of cis- and trans-[PtCl₂(NH₃)₂] with reduced glutathione, studied by ¹H, ¹³C, ¹⁹⁵Pt and ¹⁵N-{¹H} DEPT NMR. *J Inorg Biochem* 38:305–326
- Braddock PD, Connors TA, Jones M, Khokhar AR, Melzack DH, Tobe ML (1975) Structure and activity relationships of platinum complexes with anti-tumour activity. *Chem-Biol Interact* 11:145–161
- Brady HR, Kone BC, Stromski ME, Zeidel ML, Giebisch G, Gullans SR (1990) Mitochondrial injury: an early event in cisplatin toxicity to renal proximal cells. *Am J Physiol* 258:F1181–F1187
- Cohen GM (1997) Caspases: the executioners of apoptosis. *Biochem J* 326:1–16
- Corden BJ, Fine RL, Ozols RF, Collins JM (1985) Clinical pharmacology of high-dose cisplatin. *Cancer Chemother Pharmacol* 14:38–41
- Dabrowiak JC, Goodisman J, Souid A-K (2002) Kinetic study of the reaction of cisplatin with thiols. *Drug Metabol Dispos* 30:1378–1384
- Dedon PC, Borch RF (1987) Characterization of the reactions of platinum antitumor agents with biologic and non-biologic sulfur-containing nucleophiles. *Biochem Pharmacol* 36:1955–1964
- Ehrsson H, Wallin I, Yachnin J (2002) Pharmacokinetics of oxaliplatin in humans. *Med Oncol* 19:261–265
- Gao W-G, Pu S-P, Liu W-P, Liu Z-D, Yang Y-K (2003) The aqation of oxaliplatin and the effect of acid. *Acta Pharmaceutica Sinica* 38:223–226
- Gelasco A, Lippard SJ (1999) Anticancer activity of cisplatin and related compounds. *Top Biol Inorg Chem* 1:1–43
- Go RS, Adjei AA (1999) Review of the comparative pharmacology and clinical activity of cisplatin and carboplatin. *J Clin Oncol* 17:409–422
- Gong J, Traganos F, Darzynkiewicz Z (1994) A selective procedure for DNA extraction from apoptotic cells applicable for gel electrophoresis and flow cytometry. *Anal Biochem* 218:314–319
- Gonzalez VM, Fuertes MA, Alonso C, Perez JM (2001) Is cisplatin-induced cell death always produced by apoptosis? *Mol Pharmacol* 59:657–663
- Green TJ, Wilson DF, Vanderkooi JM, DeFeo AP (1988) Phosphorimeters for analysis of decay profiles and real time monitoring of exponential decay and oxygen concentrations. *Anal Biochem* 174:73–79
- Hagman D, Goodisman J, Dabrowiak JC, Souid A-K (2003) Kinetic study on the reaction of cisplatin with metallothionein. *Drug Metabol Dispos* 31:916–923
- Hagman D, Goodisman J, Souid A-K (2004) Kinetic study on the reaction of platinum drugs with glutathione. *J Pharmacol Exp Therap* 308:658–666
- Hengartner MO (2000) The biochemistry of apoptosis. *Nature* 407:770–776
- Henkle KM, Turchi JJ (1997) Induction of apoptosis in cisplatin-sensitive and -resistant human ovarian cancer cell lines. *Cancer Res* 57:4488–4497
- Johnson SW, Swiggard PA, Handel LM, Brennan JM, Godwin AK, Ozols RF, Hamilton TC (1994) Relationship between platinum-DNA adduct formation and cisplatin cytotoxicity in cisplatin-sensitive and -resistant human ovarian cancer cells. *Cancer Res* 54:5911–5916
- Kartalou M, Essigmann JM (2001) Mechanisms of resistance to cisplatin. *Mutation Res* 478:23–43
- Knox RJ, Friedlos F, Lydall DA, Roberts JJ (1986) Mechanism of cytotoxicity of anticancer platinum drugs: Evidence that cis-diamminedichloroplatinum(II) and cis-diammine(1,1-cyclobutanedicarboxylato)platinum(II) differ only in the kinetics of their interaction with DNA. *Cancer Res* 46:1972–1979

23. Kollmannsberger C, Rich O, Derigs H-G, Schleucher N, Schoffski P, Beyer J, Schoch R, Sayer HG, Gerl M, Kuczyk C, Spott C, Kanz L, Bokemeyer C (2002) Activity of oxaliplatin in patients with relapsed or cisplatin-refractory germ cell cancer: a study of the German Testicular Cancer Study Group. *J Clin Oncol* 20:2031–2037
24. Kraker A, Schmidt J, Krezoski S, Petering DH (1985) Binding of cis-dichlorodiammine platinum (II) to metallothionein in Ehrlich cells. *Biochem Biophys Res Commun* 31:786–792
25. Kruidering M, Water BVD, Heer ED, Mulder GJ, Nagelkerke JF (1997) Cisplatin-induced nephrotoxicity in porcine proximal tubular cells: mitochondrial dysfunction by inhibition of complexes I to IV of the respiratory chain. *J Pharmacol Exp Ther* 280:638–649
26. Lau AH (1999) Apoptosis induced by cisplatin nephrotoxic injury. *Kidney Int* 56:1295–1298
27. Li P, Nijhawan D, Budihardjo I, Srinivasula SM, Ahmad M, Alnemri ES, Wang X (1997) Cytochrome c and dATP-dependent formation of Apaf-1/caspase-9 complex initiates an apoptotic protease cascade. *Cell* 91:479–489
28. Liu J, Kraut E, Bender J, Brooks R, Balcerzak S, Grever M, Stanley H, D'Ambrosio S, Gibson-D'Ambrosio R, Chan KK (2002) Pharmacokinetics of oxaliplatin (NSC 266046) alone and in combination with paclitaxel in cancer patients. *Cancer Chemo Pharmacol* 49:367–374
29. Lynn NN, Howe MC, Hale RJ, Collins GN, O'Reilly PH (2003) Over-expression of metallothionein predicts resistance of transitional cell carcinoma of bladder to intravesical mitomycin therapy. *J Urol* 169:721–723
30. Nagata S (2000) Apoptotic DNA fragmentation. *Exper Cell Res* 256:12–18
31. Neidle S, Ismail IM, Sadler PJ (1980) The structure of the antitumor complex cis-(diammine)(1,1-cyclobutanedicarboxylato)Pt(II): X ray and nmr studies. *J Inorg Biochem* 13:205–212
32. Oguri S, Sakakibara T, Mase H, Shimizu T, Ishikawa K, Kimura K, Smyth RD (1988) Clinical pharmacokinetics of carboplatin. *J Clin Pharmacol* 28:208–215
33. Pattanaik A, Bachowski G, Laib J, Lemkuil D, Shaw III F, Petering DH, Hitchcock A, Saryan L (1992) Properties of the reaction of cis-dichlorodiammineplatinum (II) with metallothionein. *J Biol Chem* 267:16121–16128
34. Pendyala L, Creaven PJ (1993) In vitro cytotoxicity, protein binding, red blood cell partitioning and biotransformation of oxaliplatin. *Cancer Res* 53:5970–5976
35. Petit PX, Zamzami N, Vayssiere JL, Mignotte B, Kroemer G, Castedo M (1997) Implication of mitochondria in apoptosis. *Mol Cell Biochem* 174:185–188
36. Prenzler PD, McFadyen WD (1997) Reactions of cisplatin and the cis-diamminediaqua platinum(II) cation with Tris and Hepes. *J Inorg Biochem* 68:279–282
37. Raymond E, Faivre S, Chaney S, Woynarowski J, Cvitkovic C (2002) Cellular and molecular pharmacology of oxaliplatin. *Mol Cancer Therap* 1:227–235
38. Reedijk J, Teuben JM (1999) Platinum-sulfur interactions involved in antitumor drugs, rescue agents and biomolecules. In: Lippert B (ed) *Cisplatin, chemistry and biochemistry of a leading anticancer drug*. Weinheim Wiley-VCH, Zurich, pp 319–362
39. Robson T, Hall A, Lohrer H (1992) Increased sensitivity of a Chinese hamster ovary cell line to alkylating agents after overexpression of the human metallothionein II-A gene. *Mutation Res* 274:177–185
40. Sadowitz PD, Hubbard BA, Dabrowski JC, Goodisman J, Tacka KA, Aktas MK, Cunningham MJ, Dubowy RL, Souid A-K (2002) Kinetics of cisplatin binding to cellular DNA and modulations by thiol-blocking agents and thiol drugs. *Drug Metabol Dispos* 30:183–190
41. Saika T, Tsushima T, Ochi J, Akebi N, Nau Y, Matsumura Y, Ohmori H (1994) Over-expression of metallothionein and drug-resistance in bladder cancer. *Internat J Urol* 1:135–139
42. Souid A-K, Tacka KA, Galvan KA, Penefsky HS (2003) Immediate effects of anticancer drugs on mitochondrial oxygen consumption. *Biochem Pharmacol* 66:977–987
43. Souid A-K, Dubowy RL, Blaney SM, Hershon L, Sullivan J, McLeod WD, Bernstein ML (2003) Phase I clinical and pharmacologic study of weekly cisplatin and irinotecan combined with amifostine for refractory solid tumors: Children's Oncology Group trial 9970. *Clin Cancer Res* 9:703–710
44. Tacka KA, Dabrowski JC, Goodisman J, Penefsky HS, Souid A-K (2004) Quantitative studies on cisplatin-induced cell death. *Chem Res Toxicol* 17:1102–1111
45. Tacka KA, Szalda D, Souid A-K, Goodisman J, Dabrowski JC (2004) Experimental and theoretical studies on the pharmacodynamics of cisplatin in Jurkat cells. *Chem Res Toxicol* 17:1434–1444
46. Vaisman A, Lim SE, Patrick SM, Copeland WC, Hinkle DC, Tuchi JJ, Chaney SG (1999) Effect of DNA polymerases and high mobility group protein 1 on the carrier ligand specificity for translesion synthesis past platinum-DNA adducts. *Biochem* 38:11026–11039
47. Verstraete S, Heudi O, Cailleux A, Allain P (2001) Comparison of the reactivity of oxaliplatin, Pt(diaminocyclohexane)Cl₂ and Pt(diaminocyclohexane)(OH)₂²⁺ with guanosine and L-methionine. *J Inorg Biochem* 84:129–135
48. Wyllie AH (1980) Glucocorticoid-induced thymocyte apoptosis is associated with endogenous endonuclease activation. *Nature (London)* 284:555–556
49. Yang YY, Robbins PD, Lazo JS (1998) Differential transactivation of human metallothionein-III in cisplatin-resistant and -sensitive cells. *Oncol Res* 10:85–98
50. Zamble DB, Lippard SJ (1999) The response of cellular proteins to cisplatin-damaged DNA. In: Lippert B (ed) *Cisplatin Chemistry and Biochemistry of a Leading Anticancer Drug*. Weinheim Wiley-VCH, Zurich, pp 73–110
51. Zhang B, Tang W (1994) Kinetics of the reaction of platinum(II) complexes with metallothionein. *J Inorg Biochem* 56:143–153